

Dynamical Transition of Quantum Vortex-Pair Annihilation in a Bose-Einstein Condensate

Toshiaki Kanai¹ and Chuanwei Zhang^{1,*}

¹*Department of Physics, Washington University, St. Louis, Missouri 63130, USA*

Understanding the elementary mechanism for the dissipation of vortex energy in quantum liquids is one central issue in quantum hydrodynamics, such as quantum turbulence in systems ranging from neutron stars to atomic condensates. In a two-dimensional (2D) Bose-Einstein condensate (BEC) at zero temperature, besides the vortex drift-out process from the boundary, vortex-antivortex pair can annihilate in the bulk, but controversy remains on the number of vortices involved in the annihilation process. We find there exists a dynamical transition from four-body to three-body vortex annihilation processes with the time evolution in a boundary-less uniform quasi-2D BEC. Such dynamical transition depends on the initial vortex pair density, and occurs when the sound waves generated in the vortex annihilation process surpass a critical energy. With the confinement along the third direction is relaxed in a quasi-2D BEC, the critical sound wave energy decreases due to the 3D vortex line curve and reconnection, shifting the dynamical transition to the early time. Our work reveals an elementary mechanism for the dissipation of vortex energy that may help understand exotic matter and dynamics in quantum liquids.

Quantum vortices, ubiquitous topological excitations, play an important role in diverse quantum phenomena such as Berezinskii-Kosterlitz-Thouless transition [1–6], Kibble–Zurek mechanism [7–14], and quantum turbulence [15]. In quantum liquids, the quantization of the superflow circulation around the vortex makes the vorticity robust against decay. The understanding of vortex motion and their decaying mechanism is thus fundamentally important and has attracted much attention recently, particularly in 2D quantum turbulence [16–32]. In a 2D BEC, quantum vortices may disappear via two processes: vortex drifting-out from the boundary and vortex-pair annihilation in the bulk [33]. Here the vortex pair represents a pair of vortex and antivortex with positive and negative single quantum of circulations.

So far the basic mechanism for the vortex-pair annihilation remains inconclusive. While vortex-pair annihilation was initially considered as a two-body process [33, 34], later studies utilizing the purely 2D Gross-Pitaevskii equation (GPE) showed that it is a four-body process at zero temperature [20, 21, 35], where the vortex pair forms a soliton-like structure [36–39] (i.e., a pair with a short vortex distance) through a three-body interaction with the third vortex. This soliton-like structure is robust, and the fourth vortex is needed to dissipate it to sound waves, as illustrated in Fig. 1(a). However, recent work utilizing 3D GPE demonstrated that the vortex-pair annihilation is a three-body process (Fig. 1(b)) in a uniform quasi-2D BEC [40] with a strong confinement along the third direction. These different results raise the natural question regarding the fundamental mechanism behind the vortex-pair annihilation, particularly in the dimensional crossover from 2D to 3D for a realistic quasi-2D BEC.

In this Letter, we address this important question by simulating vortex decay dynamics in a boundary-less uniform quasi-2D BEC utilizing the 3D GPE with different confinements along the third direction. Here the

boundary-less condition prohibits the vortex drifting-out process in the 2D plane. Our main results are:

- i) The vortex annihilation process is governed by the sound wave intensity characterized by a critical energy

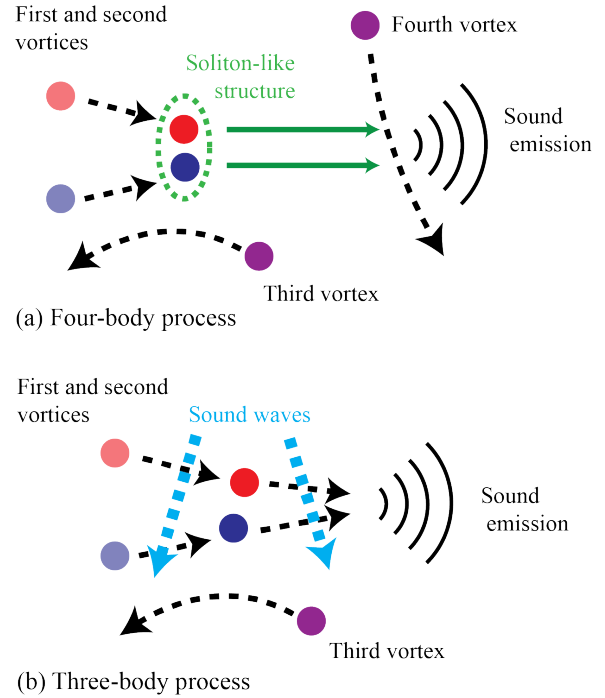


FIG. 1. Schematics of the vortex-pair annihilation process. (a) Four-body process: the first and second vortices form a soliton-like structure. The third vortex is needed to conserve the vortex energy and momentum. This soliton-like structure is robust in uniform 2D BECs, and the fourth vortex is required to break the structure into sound waves. (b) Three-body process: the pair of the first and second vortices dissipates to sound waves via the interaction with the third vortex and sound waves.

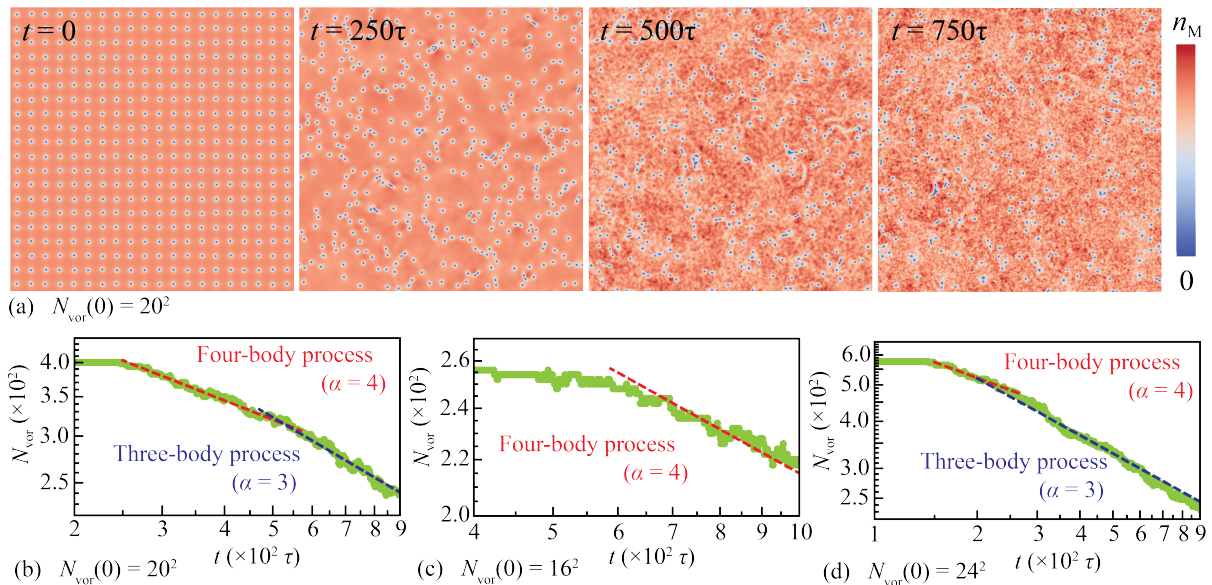


FIG. 2. (a) Snapshots of density profile in a representative case with $L_z = 2\xi$ and the initial vortex number $N_{\text{vor}}(0) = 20^2$. These plots are on the cross-section at $z = 0$. The maximum value of the color bar is $n_M = 2 \times 10^{-5} N/\xi^3$. (b-d) Time evolution of the vortex number decay. The initial vortex number is $N_{\text{vor}}(0) = 20^2$ (b), $N_{\text{vor}}(0) = 16^2$ (c), and $N_{\text{vor}}(0) = 24^2$ (d). The red and blue dashed lines correspond to four-body and three-body processes, respectively.

E_c , below (above) which the annihilation process is four-body (three-body). With a low initial vortex density, the vortex-pair annihilation remains a four-body process during the dynamical evolution due to the low sound wave energy generated in the annihilation process.

ii) In the high initial vortex density region, the vortex annihilation starts from the four-body process. However, the generated sound wave energy from the vortex annihilation exceeds E_c after certain time t , leading to a dynamical transition [41] from four-body to three-body processes.

iii) The critical sound wave energy decreases for weakening confinement along the third direction. As the confinement becomes weaker, the vortex lines can curve and reconnect along the third dimension, which reduce the effective critical sound wave energy for annihilating the vortex pairs, shifting the dynamical transition to an early time.

Description of a quasi-2D BEC and numerical method. We simulate the dynamics of a quasi-2D BEC by the 3D GPE [42]:

$$i\hbar \frac{\partial \Psi(\mathbf{r}, t)}{\partial t} = -\frac{\hbar^2}{2m} \nabla^2 \Psi + U(z)\Psi + C|\Psi|^2\Psi - \mu\Psi, \quad (1)$$

where Ψ is the macroscopic wave function, \hbar is the reduced Plank constant, m is the atom mass, and $C = 4\pi\hbar^2 a_s/m$ is the interaction strength with the s -wave scattering length a_s . For simplicity, we assume the quasi-2D BEC

is confined in the z -direction by a box potential

$$U(z) = \begin{cases} \infty & |z| \geq L_z/2 \\ 0 & |z| < L_z/2. \end{cases} \quad (2)$$

The periodic boundary condition is assumed in the x - y plane so that quantum vortices may disappear only through the vortex-pair annihilation process. Kelvin waves, *i.e.*, transverse excitations along a vortex line, are suppressed in thin BECs with a small L_z [43], and such suppression is often considered as the criteria of 2D in the context of quantum turbulence [44].

The BEC density n is given by $n = |\Psi|^2$, and the velocity field \mathbf{v} is computed by $\mathbf{v}(\mathbf{r}, t) = \frac{\hbar}{2mi} \frac{\Psi^* \nabla \Psi - \Psi \nabla \Psi^*}{n}$. The BEC dynamics has the healing length scale $\xi = \hbar/\sqrt{2m\mu_0}$ and time scale $\tau = \hbar/\mu_0$ with the equilibrium chemical potential $\mu_0 = Cn_0$ and the average BEC density n_0 . We solve the GPE by the fourth-order Runge-Kutta-Gill's method [45] with the spatial step $\Delta x = 0.25\xi$ and the time step $\Delta t = 0.1 \times 0.25^2\tau$. The computational domain size is $L_x \times L_y \times L_z = [0, 256\xi] \times [0, 256\xi] \times [-L_z/2, L_z/2]$. In our simulations, L_z varies from ξ to 8ξ , which are thin enough for the 2D criteria. For the initial state, we arrange $N_{\text{vor}}(0)/2$ positive and $N_{\text{vor}}(0)/2$ negative vortices alternatively as a square lattice in the x - y plane, yielding the vortex density $N_{\text{vor}}(0)/(256\xi)^2$. To reduce the initial density fluctuations, we generate the initial state by the imaginary time evolution with the pinning potential located at vortex locations, hence the initial state has no sound waves [46].

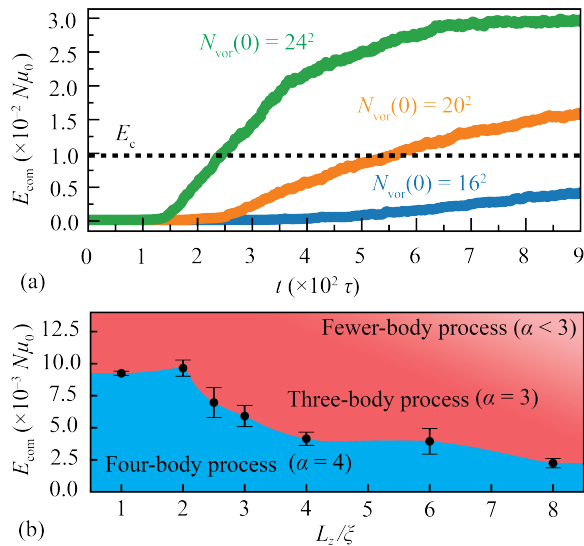


FIG. 3. (a) Time evolution of the compressible kinetic energy E_{com} with various initial vortex numbers $N_{\text{vor}}(0)$ under the same $L_z = 2\xi$. The dashed line represents the critical energy E_C determined from $N_{\text{vor}}(0) = 20^2$. The three-body scaling is observed when $E_{\text{com}} > E_C$. (b) Dependence of E_C on the z -axis confinement L_z . $N_{\text{vor}}(0) = 20^2$. The boundary between three and four-body processes is drawn for illustration by connecting E_C . With larger E_{com} , the vortex-pair annihilation may involve the two-body process, where α is smaller than 3.

Dynamical transition from four-body to three-body processes. Fig. 2 (a) shows the density evolution of a BEC with $L_z = 2\xi$ and the initial vortex number $N_{\text{vor}}(0) = 20^2$. At $t = 0$, the BEC has no sound waves, and the vortices are placed as a square lattice with the lattice constant $\sqrt{L_x L_y / N_{\text{vor}}} = 256\xi/20$. Here we slightly shift the vortices randomly to break the discrete translational symmetry. As the BEC evolves, the vortex pairs annihilate, emitting sound waves. The sound waves are less in the early time $t = 250\tau$, but the BEC becomes strongly wavy in a later time $t = 750\tau$.

The number of vortices involved in the vortex decay process can be characterized by the scaling of the vortex number decay [21, 35]. For a α -body vortex decay process, the rate equation of the vortex number N_{vor} is given by

$$\frac{dN_{\text{vor}}(t)}{dt} \propto -N_{\text{vor}}^\alpha, \quad (3)$$

therefore the vortex number scales as

$$N_{\text{vor}}(t) \propto t^{-1/(\alpha-1)}. \quad (4)$$

Fig. 2(b) shows the vortex number decay corresponding to Fig. 2(a). After vortex pairs start to annihilate, the vortex number follows the scaling $N_{\text{vor}}(t) \propto t^{-1/3}$ at the early time, corresponding to the four-body process. After certain time of evolution, the vortex number scaling changes to $N_{\text{vor}} \propto t^{-1/2}$, corresponding to the three-body

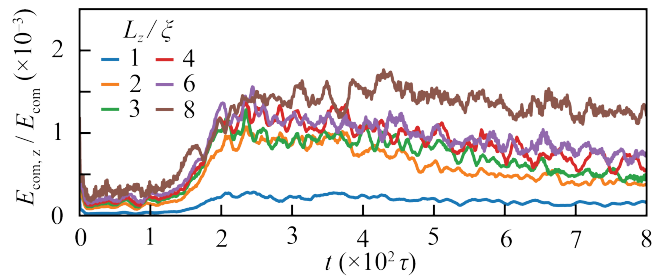


FIG. 4. Time evolution of the fraction of the z component contribution $E_{\text{com},z}/E_{\text{com}}$ with various confinement L_z .

process. The transition depends on the initial vortex number (i.e., vortex density): there is only four-body process for $N_{\text{vor}}(0) = 16^2$ (Fig. 2(c)), while the transition occurs earlier for $N_{\text{vor}}(0) = 24^2$ (Fig. 2(d)). Such dynamical transition from four-body to three-body processes have not been discussed before and understanding the mechanism behind it is the main focus hereafter.

Dynamical transition induced by increasing sound waves. At finite temperatures, the thermal excitations dampening the kinetic energy may change the scaling of N_{vor} [21, 35], but the GPE model here has no thermal excitations. Sound waves can extract energy from quantum vortices [36], and a complementary test of vortex-pair annihilation shown later verifies the damping effect. In our case, intense sound waves generated by the pair-annihilation in the early stage dampen the vortex energy later, varying the scaling to a three-body process illustrated in Fig. 1(b).

To characterize the sound wave intensity, we decompose the velocity field as $\mathbf{v} = \mathbf{v}_{\text{com}} + \mathbf{v}_{\text{inc}}$ with the incompressible velocity \mathbf{v}_{inc} and the compressible velocity \mathbf{v}_{com} , satisfying $\nabla \cdot (\sqrt{n}\mathbf{v}_{\text{inc}}) = 0$ and $\nabla \times (\sqrt{n}\mathbf{v}_{\text{com}}) = 0$, respectively. Then the compressible kinetic energy E_{com} and the incompressible kinetic energy E_{inc} can be computed by [47–49]

$$E_{\text{com}} = \frac{m}{2} \int n |\mathbf{v}_{\text{com}}|^2 dV \quad (5)$$

$$E_{\text{inc}} = \frac{m}{2} \int n |\mathbf{v}_{\text{inc}}|^2 dV. \quad (6)$$

E_{com} and E_{inc} are associated with sound waves and vortices, respectively [48, 49]. Fig. 3 (a) shows the E_{com} evolution with various initial vortex numbers. E_{com} steadily increases as more vortex-pairs annihilate. In the case of $N_{\text{vor}}(0) = 20^2$, the three-body process emerges after about $t = 520\tau$, when the compressible kinetic energy is about $E_{\text{com}} \approx 9.7 \times 10^{-3} N\mu_0$ with the total particle number $N = \int n dV$. This compressible kinetic energy is defined as the critical energy E_C . With $N_{\text{vor}}(0) = 16^2$, E_{com} is always lower than E_C in our simulation, and the scaling of N_{vor} follows the four-body process during the evolution (Fig. 2 (c)). For $N_{\text{vor}}(0) = 24^2$, E_{com} quickly increases and becomes higher than E_C , inducing

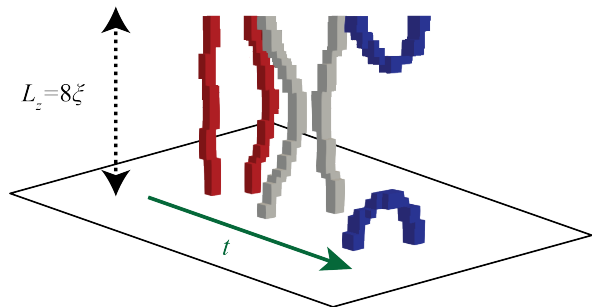


FIG. 5. Vorticity evolution of a vortex reconnection event in a BEC simulation. $L_z = 8\xi$. The red, white, and blue lines represent the vorticity at $t = 350\tau$, 355τ , and 360τ , respectively.

the dynamical transition early in time (Fig. 2 (d)). E_C is estimated from $N_{\text{vor}}(0) = 20^2$ but matches the transition time for $N_{\text{vor}}(0) = 24^2$, indicating that the critical energy is mostly independent of the initial vortex number in our parameter range.

Confinement dependence in the quasi-2D BEC. When L_z increases, we expect a crossover from 2D to quasi-2D and then 3D for the BEC. For each L_z , we sample three cases from different initial states with the same initial vortex number $N_{\text{vor}}(0) = 20^2$ and compute the arithmetic-averaged critical energy \bar{E}_C shown in Fig. 3 (b). We see \bar{E}_C is almost a constant below $L_z = 2\xi$ and starts decreasing beyond $L_z = 2\xi$. The decrease of \bar{E}_C cannot attribute to Kelvin waves since they are still suppressed even for $L_z = 8\xi$. One intuitive guess is the increase of the sound waves in the z -direction, which may be evaluated by the compressible kinetic energy in the z -direction $E_{\text{com},z} = \frac{m}{2} \int n |\mathbf{v}_{\text{com}} \cdot \hat{\mathbf{e}}_z|^2 dV$ with the unit vector in the z -direction $\hat{\mathbf{e}}_z$. Fig. 3 (b) shows the fraction $E_{\text{com},z}/E_{\text{com}}$. In our parameter range $\xi \leq L_z \leq 8\xi$, $E_{\text{com},z}$ is always less than 0.2% of E_{com} , demonstrating that the z -component of sound waves is negligible. Therefore, the change of the critical energy should come from the vortex contribution.

We find that the decrease of \bar{E}_C with increasing L_z is due to the emergence of vortex reconnection channel. As L_z increases, vortices can be easily curved, and the vortex distance may vary in the z -direction. Thus the soliton-like structure becomes unstable, enhancing the vortex reconnection channel that makes the sound wave easier to annihilate the vortex pair. Fig. 5 shows snapshots of a vortex reconnection event in a BEC with $L_z = 8\xi$. To quantitatively characterize this effect, we analyze the incompressible kinetic energy of the z -component

$$E_{\text{inc},z} = \frac{m}{2} \int n |\mathbf{v}_{\text{inc}} \cdot \hat{\mathbf{e}}_z|^2 dV. \quad (7)$$

If the vortices do not curve, the incompressible velocity is confined in the x - y plane, and $E_{\text{inc},z}$ is negligible. Fig. 6 (a) shows the time evolution of the ratio between $E_{\text{inc},z}$

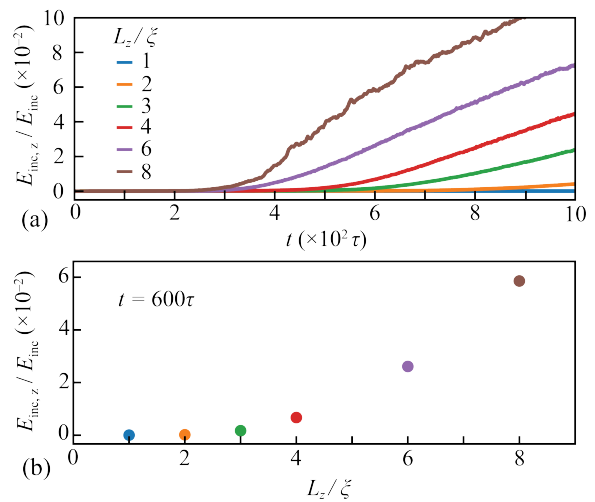


FIG. 6. (a) Time evolution of the fraction of the z component contribution $E_{\text{inc},z}/E_{\text{inc}}$ with various L_z for $N_{\text{vor}} = 20^2$. (b) Dependence of the fraction $E_{\text{inc},z}/E_{\text{inc}}$ on L_z at $t = 600\tau$.

and E_{inc} , which can be over 10% with $L_z = 8\xi$ that is a significant contribution. Fig. 6 (b) shows the L_z dependence of the ratio at $t = 600\tau$. The contribution of the z -component is suppressed below $L_z = 2\xi$ and rapidly increases above $L_z = 3\xi$. This result means that the vortex reconnection effect becomes significant above $L_z = 3\xi$, agreeing with the observation in the critical energy observed in Fig. 3 (b).

Complementary test of vortex-pair annihilation by sound waves. To directly demonstrate the energy damping caused by sound waves, the dynamics of a vortex-pair are analyzed for different cases. In case 1, the initial BEC has no sound waves, and we implement a vortex-pair with a vortex distance $d_V(t=0) = 3.5\xi$. Here the initial density profile is given by the two-point Padé approximation [50]. In case 2, the BEC contains the compressible kinetic energy $E_{\text{com}} \approx 2.5 \times 10^{-2} N\mu_0$, which is high enough so that the vortex-pair annihilation may be a three-body process. We then implement a vortex-pair in the same way as case 1. Fig. 7 shows the time evolution of the vortex distance $d_V(t)$, which is associated with the vortex energy. $d_V(t)$ is almost constant in case 1, but rapidly varies over a short period and gradually decays over a long time in case 2, indicating that sound waves may fluctuate the vortex-pair energy and gradually dissipate it. Note that the energy dissipation due to sound waves does not need to be strong enough to dampen out the vortex-pair energy by itself since their role is to destabilize the metastable state. In fact, weak energy dissipation of thermal excitations' scattering may alter the vortex-pair annihilation to a two-body process [21, 35].

Discussion and conclusion. Past studies utilizing the 2D GPE used relatively low initial vortex densities, therefore the three-body process does not emerge (e.g., $N_{\text{vor}}(0)/(L_x L_y) = 10^3/10^4 \xi^{-2} \approx 153/256^2 \xi^{-2}$ in [35]).

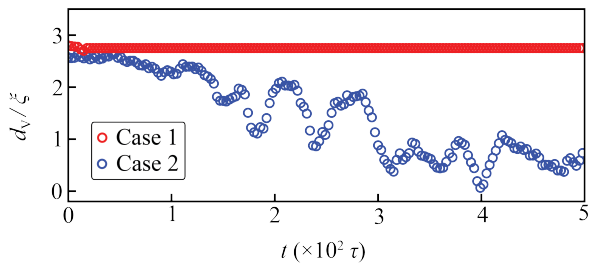


FIG. 7. Time evolution of the vortex distance $d_V(t)$ in two cases. Case 1 has no initial sound waves, and case 2 has intense sound waves of the compressible kinetic energy $E_C \approx 2.5 \times 10^{-2} N \mu_0$ at $t = 0$. $L_z = 4\xi$. Here d_V is computed for every t , and a moving average is taken within $[t - 10\tau, t + 10\tau]$.

On the other hand, the 3D GPE study of the quasi-2D BEC [40] did not observe the four-body process because of the relatively weak confinement in the third direction, leading to a very small critical energy. As a result, the vortex decay dynamics quickly pass the transition point from four-body to three-body processes at an early time.

Our simulations focus on the dynamics at the absolute zero temperature, but rich physics is expected at finite temperatures due to the scattering with thermal excitations [21, 35]. Quasi-2D BECs have been realized in many experiments [2, 51] with the tunable third dimension confinement. The uniform BEC on the 2D plane can be achieved using the box types of potential [52, 53]. It is also worth noting that vortex collision can be controlled by localized optical potentials [54], which allow us to measure the sound wave dissipation to the vortex-pair directly and locally.

In summary, we have demonstrated that the vortex-pair annihilation process undergoes a dynamical transition from four-body to three-body processes due to increasing sound waves generated in annihilation process in the early stage. We characterize the role of the initial vortex density and the third dimension confinement in the quasi-2D BEC for such dynamical transition. Our work reveals an elementary mechanism for vortex energy dissipation through pairing annihilation that has been a long-standing issue in the field. Understanding such vortex dissipation dynamics allows better characterization of dynamical phenomena (e.g., quantum turbulence) of quantum liquids for new quantum technologies applications.

Acknowledgement: The authors acknowledge the support of the Air Force Office of Scientific Research under Grant No. FA9550-20-1-0220 and the National Science Foundation under Grant No. PHY-2409943, OSI-2228725, ECCS-2411394.

* Email: chuanwei.zhang@wustl.edu

[1] S. Stock, Z. Hadzibabic, B. Battelier, M. Cheneau, and

- J. Dalibard, Observation of Phase Defects in Quasi-Two-Dimensional Bose-Einstein Condensates, *Phys. Rev. Lett.* **95**, 190403 (2005).
- [2] Z. Hadzibabic, P. Krüger, M. Cheneau, B. Battelier, and J. Dalibard, Berezinskii-Kosterlitz-Thouless crossover in a trapped atomic gas, *Nature* **441**, 1118-1121 (2006).
- [3] V. Schweikhard, S. Tung, and E. A. Cornell, Vortex Proliferation in the Berezinskii-Kosterlitz-Thouless Regime on a Two-Dimensional Lattice of Bose-Einstein Condensates, *Phys. Rev. Lett.* **99**, 030401 (2007).
- [4] P. Krüger, Z. Hadzibabic, and J. Dalibard, Critical Point of an Interacting Two-Dimensional Atomic Bose Gas, *Phys. Rev. Lett.* **99**, 040402 (2007).
- [5] S. Nazarenko, M. Onorato, and D. Proment, Bose-Einstein condensation and Berezinskii-Kosterlitz-Thouless transition in the two-dimensional nonlinear Schrödinger model, *Phys. Rev. A* **90**, 013624 (2014).
- [6] S. Sunami, V. P. Singh, D. Garrick, A. Beregi, A. J. Barker, K. Luksch, E. Bentine, L. Mathey, and C. J. Foot, Observation of the Berezinskii-Kosterlitz-Thouless Transition in a Two-Dimensional Bose Gas via Matter-Wave Interferometry, *Phys. Rev. Lett.* **128**, 250402 (2022).
- [7] D. R. Scherer, C. N. Weiler, T. W. Neely, and B. P. Anderson, Vortex Formation by Merging of Multiple Trapped Bose-Einstein Condensates, *Phys. Rev. Lett.* **98**, 110402 (2007).
- [8] C. N. Weiler, T. W. Neely, D. R. Scherer, A. S. Bradley, M. J. Davis, and B. P. Anderson, Spontaneous vortices in the formation of Bose-Einstein condensates, *Nature* **455**, 948-951 (2008).
- [9] T. Kanai, W. Guo, and M. Tsubota, Flows with fractional quantum circulation in Bose-Einstein condensates induced by nontopological phase defects, *Phys. Rev. A* **97**, 013612 (2018).
- [10] T. Kanai, W. Guo, and M. Tsubota, Merging of Rotating Bose-Einstein Condensates, *J. Low Temp. Phys.* **195**, 37-50 (2019).
- [11] B. Ko, J. W. Park, and Y. Shin, Kibble-Zurek universality in a strongly interacting Fermi superfluid, *Nat. Phys.* **15**, 1227-1231 (2019).
- [12] T. Kanai, W. Guo, M. Tsubota, and D. Jin, Torque and Angular-Momentum Transfer in Merging Rotating Bose-Einstein Condensates, *Phys. Rev. Lett.* **124**, 105302 (2020).
- [13] J. Goo, Y. Lim, and Y. Shin, Defect Saturation in a Rapidly Quenched Bose Gas, *Phys. Rev. Lett.* **127**, 115701 (2021).
- [14] J. Rysti, J. T. Mäkinen, S. Autti, T. Kamppinen, G. E. Volovik, and V. B. Eltsov, Suppressing the Kibble-Zurek Mechanism by a Symmetry-Violating Bias, *Phys. Rev. Lett.* **127**, 115702 (2021).
- [15] C. F. Barenghi, L. Skrbek, and K. R. Sreenivasan, *Quantum turbulence*, (Cambridge University Press, Cambridge, 2024).
- [16] J. Schole, B. Nowak, and T. Gasenzer, Critical dynamics of a two-dimensional superfluid near a nonthermal fixed point, *Phys. Rev. A* **86**, 013624 (2012).
- [17] T. P. Billam, M. T. Reeves, B. P. Anderson, and A. S. Bradley, Onsager-Kraichnan Condensation in Decaying Two-Dimensional Quantum Turbulence, *Phys. Rev. Lett.* **112**, 145301 (2014).
- [18] T. Simula, M. J. Davis, and K. Helmersson, Emergence of Order from Turbulence in an Isolated Planar Superfluid, *Phys. Rev. Lett.* **113**, 165302 (2014).

- [19] A. Lucas and P. Surówka, Sound-induced vortex interactions in a zero-temperature two-dimensional superfluid, *Phys. Rev. A* **90**, 053617 (2014).
- [20] A. Cidrim, F. E. A. dos Santos, L. Galantucci, V. S. Bagnato, and C. F. Barenghi, Controlled polarization of two-dimensional quantum turbulence in atomic Bose-Einstein condensates, *Phys. Rev. A* **93**, 033651 (2016).
- [21] A. J. Groszek, T. P. Simula, D. M. Paganin, and K. Helmerson, Onsager vortex formation in Bose-Einstein condensates in two-dimensional power-law traps, *Phys. Rev. A* **93**, 043614 (2016).
- [22] X. Yu, T. P. Billam, J. Nian, M. T. Reeves, and A. S. Bradley, Theory of the vortex-clustering transition in a confined two-dimensional quantum fluid, *Phys. Rev. A* **94**, 023602 (2016).
- [23] S. W. Seo, B. Ko, J. H. Kim, and Y. Shin, Observation of vortex-antivortex pairing in decaying 2D turbulence of a superfluid gas, *Sci. Rep.* **7**, 4587 (2017).
- [24] M. Karl and T. Gasenzer, Strongly anomalous non-thermal fixed point in a quenched two-dimensional Bose gas, *New J. Phys.* **19**, 093014 (2017).
- [25] A. J. Groszek, M. J. Davis, D. M. Paganin, K. Helmerson, and T. P. Simula, Vortex Thermometry for Turbulent Two-Dimensional Fluids, *Phys. Rev. Lett.* **120**, 034504 (2018).
- [26] A. Frishman and C. Herbert, Turbulence Statistics in a Two-Dimensional Vortex Condensate, *Phys. Rev. Lett.* **120**, 204505 (2018).
- [27] G. Gauthier, M. T. Reeves, X. Yu, A. S. Bradley, M. A. Baker, T. A. Bell, H. Rubinsztein-Dunlop, M. J. Davis, and T. W. Neely, Giant vortex clusters in a two-dimensional quantum fluid, *Science* **364**, 1264-1267 (2019).
- [28] S. P. Johnstone, A. J. Groszek, P. T. Starkey, C. J. Billington, T. P. Simula, and K. Helmerson, Evolution of large-scale flow from turbulence in a two-dimensional superfluid, *Science* **364**, 1267-1271 (2019).
- [29] Y. P. Sachkou, C. G. Baker, G. I. Harris, O. R. Stockdale, S. Forstner, M. T. Reeves, X. He, D. L. McAuslan, A. S. Bradley, M. J. Davis, and W. P. Bowen, Coherent vortex dynamics in a strongly interacting superfluid on a silicon chip, *Science* **366**, 1480-1485 (2019).
- [30] A. J. Groszek, M. J. Davis, and T. P. Simula, Decaying quantum turbulence in a two-dimensional Bose-Einstein condensate at finite temperature, *SciPost Phys.* **8**, 039 (2020).
- [31] M. T. Reeves, K. Goddard-Lee, G. Gauthier, O. R. Stockdale, H. Salman, T. Edmonds, X. Yu, A. S. Bradley, M. Baker, H. Rubinsztein-Dunlop, M. J. Davis, and T. W. Neely, Turbulent Relaxation to Equilibrium in a Two-Dimensional Quantum Vortex Gas, *Phys. Rev. X* **12**, 011031 (2022).
- [32] T. Easton, M. Kokmotos, and G. Barontini, Vortex clustering in trapped Bose-Einstein condensates, *Sci. Rep.* **13**, 19432 (2023).
- [33] W. J. Kwon, G. Moon, J. Choi, S. W. Seo, and Y. Shin, Relaxation of superfluid turbulence in highly oblate Bose-Einstein condensates, *Phys. Rev. A* **90**, 063627 (2014).
- [34] G. W. Stagg, A. J. Allen, N. G. Parker, and C. F. Barenghi, Generation and decay of two-dimensional quantum turbulence in a trapped Bose-Einstein condensate, *Phys. Rev. A* **91**, 013612 (2015).
- [35] A. W. Baggaley and C. F. Barenghi, Decay of homogeneous two-dimensional quantum turbulence, *Phys. Rev. A* **97**, 033601 (2018).
- [36] S. Nazarenko and M. Onorato, Freely decaying Turbulence and Bose-Einstein Condensation in Gross-Pitaevski Model, *J. Low Temp. Phys.* **146**, 31-46 (2007).
- [37] L. A. Smirnov and V. A. Mironov, Dynamics of two-dimensional dark quasisolitons in a smoothly inhomogeneous Bose-Einstein condensate, *Phys. Rev. A* **85**, 053620 (2012).
- [38] L. A. Smirnov and A. I. Smirnov, Scattering of two-dimensional dark solitons by a single quantum vortex in a Bose-Einstein condensate, *Phys. Rev. A* **92**, 013636 (2015).
- [39] E. Rickinson, N. G. Parker, A. W. Baggaley, and C. F. Barenghi, Diffusion of quantum vortices, *Phys. Rev. A* **98**, 023608 (2018).
- [40] T. Kanai and W. Guo, True Mechanism of Spontaneous Order from Turbulence in Two-Dimensional Superfluid Manifolds, *Phys. Rev. Lett.* **127**, 095301 (2021).
- [41] T. Ma and S. Wang, *Phase Transition Dynamics*, (Springer International Publishing, Cham, 2019).
- [42] C. J. Pethick and H. Smith, *Bose-Einstein condensation in dilute gases*, 2nd ed., (Cambridge University Press, Cambridge, 2008).
- [43] S. J. Rooney, P. B. Blakie, B. P. Anderson, and A. S. Bradley, Suppression of Kelvin-induced decay of quantized vortices in oblate Bose-Einstein condensates, *Phys. Rev. A* **84**, 023637 (2011).
- [44] L. Chomaz, L. Corman, T. Bienaimé, R. Desbuquois, C. Weitenberg, S. Nascimbène, J. Beugnon, and J. Dalibard, Emergence of coherence via transverse condensation in a uniform quasi-two-dimensional Bose gas, *Nat Commun* **6**, 6162 (2015).
- [45] M. Abramowitz and I. A. Stegun (Eds.), *Handbook of mathematical functions: with formulas, graphs, and mathematical tables*, (Dover Publ, New York, NY, 2013).
- [46] R. Boral, S. Sarkar, and P. K. Mishra, Structural Transformation and Melting of the Vortex Lattice in the Rotating Bose Einstein Condensates. In: Banerjee, S., Saha, A. (eds) *Nonlinear Dynamics and Applications*. Springer Proceedings in Complexity. Springer, Cham. https://link.springer.com/10.1007/978-3-030-99792-2_106
- [47] R. Numasato, M. Tsubota, and V. S. L'vov, Direct energy cascade in two-dimensional compressible quantum turbulence, *Phys. Rev. A* **81**, 063630 (2010).
- [48] A. S. Bradley and B. P. Anderson, Energy Spectra of Vortex Distributions in Two-Dimensional Quantum Turbulence, *Phys. Rev. X* **2**, 041001 (2012).
- [49] T.-L. Horng, C.-H. Hsueh, S.-W. Su, Y.-M. Kao, and S.-C. Gou, Two-dimensional quantum turbulence in a nonuniform Bose-Einstein condensate, *Phys. Rev. A* **80**, 023618 (2009).
- [50] C. Rorai, K. R. Sreenivasan, and M. E. Fisher, Propagating and annihilating vortex dipoles in the Gross-Pitaevskii equation, *Phys. Rev. B* **88**, 134522 (2013).
- [51] C.-L. Hung, X. Zhang, N. Gemelke, and C. Chin, Observation of scale invariance and universality in two-dimensional Bose gases, *Nature* **470**, 236 (2011).
- [52] A. L. Gaunt, T. F. Schmidutz, I. Gotlibovych, R. P. Smith, Z. Hadzibabic, Bose-Einstein condensation of atoms in a uniform potential, *Phys. Rev. Lett.* **110**, 200406 (2013).
- [53] B. Mukherjee, Z. Yan, P. B. Patel, Z. Hadzibabic, T. Yefsah, J. Struck, and M. W. Zwierlein, Homogeneous Atomic Fermi Gases, *Phys. Rev. Lett.* **118**, 123401 (2017).

- [54] W. J. Kwon, G. Del Pace, K. Xhani, L. Galantucci, A. Muzi Falconi, M. Inguscio, F. Scazza, and G. Roati, Sound emission and annihilations in a programmable quantum vortex collider, *Nature* **600**, 64 (2021).